Cell PRESS
Chemistry & Biology
Article

Promysalin, a Salicylate-Containing *Pseudomonas putida* Antibiotic, Promotes Surface Colonization and Selectively Targets Other *Pseudomonas*

Wen Li,[1] Paulina Estrada-de los Santos,[1,5] Sandra Matthijs,[2,6] Guan-Lin Xie,[3] Roger Busson,[4] Pierre Cornelis,[2] Jef Rozenski,[4] and René De Mot[1,*]
[1]Centre of Microbial and Plant Genetics, Katholieke Universiteit Leuven, Heverlee-Leuven 3001, Belgium
[2]Molecular Interactions, Department of Molecular and Cellular Interactions, Flanders Institute for Biotechnology and Vrije Universiteit Brussel, Brussels 1050, Belgium
[3]Institute of Biotechnology, Zhejiang University, Hangzhou 310029, China
[4]Laboratory of Medicinal Chemistry, Rega Institute for Medical Research, Katholieke Universiteit Leuven, Leuven 3000, Belgium
[5]Present address: Centro de Ciencias Genómicas, Universidad Nacional Autónoma de México, Cuernavaca 62210, México
[6]Present address: Institut de Recherches Microbiologiques Jean-Marie Wiame, Brussels 1070, Belgium
*Correspondence: rene.demot@biw.kuleuven.be
DOI 10.1016/j.chembiol.2011.08.006

SUMMARY

Under control of the Gac regulatory system, *Pseudomonas putida* RW10S1 produces promysalin to promote its own swarming and biofilm formation, and to selectively inhibit many other pseudomonads, including the opportunistic pathogen *Pseudomonas aeruginosa*. This amphipathic antibiotic is composed of salicylic acid and 2,8-dihydroxymyristamide bridged by a unique 2-pyrroline-5-carboxyl moiety. In addition to enzymes for salicylic acid synthesis and activation, the biosynthetic gene cluster encodes divergent type II fatty acid biosynthesis components, unusual fatty acid-tailoring enzymes (two Rieske-type oxygenases and an amidotransferase), an enzyme resembling a proline-loading module of nonribosomal peptide synthetases, and the first prokaryotic member of the BAHD family of plant acyltransferases. Identification of biosynthetic intermediates enabled to propose a pathway for synthesis of this bacterial colonization factor.

INTRODUCTION

Although few commercial antibiotics originate from *Pseudomonas* (e.g., the polyketide mupirocin) (Thomas et al., 2010), studies on the biocontrol activity of plant-associated *Pseudomonas* have revealed their capacity to produce an array of antagonistic molecules to compete with other soil and rhizosphere microorganisms, in particular phytopathogenic fungi. In addition to high-affinity siderophores like pyoverdine and pyochelin, which deprive competitors from iron, antibiotics produced include phenazines, phloroglucinols, pyoluteorin, pyrrolnitrin, and cyclic lipopeptides (Haas and Défago, 2005; Raaijmakers et al., 2010). Pyrrolnitrin has served as a lead structure in the development of the phenylpyrrole class of agricultural fungicides (Ligon et al., 2000). Production of most of these *Pseudomonas* antifungal metabolites is triggered by environmental cues activating the Gac/Rsm signal transduction pathway, a global regulatory system controlling various forms of social behavior in *Pseudomonas* and many other phylogenetically related bacteria (Lapouge et al., 2008).

Antagonism among *Pseudomonas* bacteria can be mediated by different types of bacteriocins, protein toxins characterized by a narrow spectrum of activity (Michel-Briand and Baysse, 2002; Parret et al., 2005; Barreteau et al., 2009; Inglis et al., 2009; Waite and Curtis, 2009). 3-Methylarginine, mediating antagonism between two *Pseudomonas syringae* pathovars (Braun et al., 2010), represents a rare example of a secondary metabolite specifically inhibiting other *Pseudomonas*. Protegrin-based peptidomimetics specifically targeting *Pseudomonas* have been synthesized recently (Srinivas et al., 2010). Here, we report on the characterization of an intragenus-specific antibiotic, promysalin, produced under control of the Gac regulatory system. Promysalin, which also contributes to biofilm formation and is required for swarming motility of its producer, *P. putida* RW10S1, represents a new type of salicylic acid-containing molecule.

RESULTS

Intragenus-Specific Antibiotic Activity of *P. putida* RW10S1

Antagonistic activity of strain RW10S1 was observed during screening of a collection of *Pseudomonas* rhizosphere isolates from tropical crops (Vlassak et al., 1992) for bacteriocin-like activity exhibited toward other strains of the genus. Unlike *Pseudomonas* bacteriocins (Parret et al., 2003), antagonistic activity of strain RW10S1 toward other pseudomonads is neither stress enhanced by exposure of producer cells to UV light nor abolished by protease treatment. In addition, growth of many more *Pseudomonas* is inhibited than would be observed for a typical bacteriocin. Among 16 *Pseudomonas* species tested, sensitive strains were identified in 12 of these species. Remarkably, no other γ-proteobacterial species (except *Azotobacter vinelandii*) are affected nor are the strains of α- and

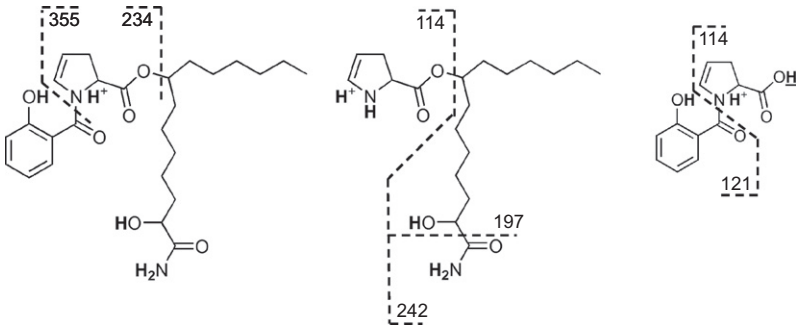

Figure 1. Main Fragments Obtained by Collision-Induced Fragmentation in a Mass Spectrometer
Hydrogens in bold are exchangeable; the underlined hydrogen is partially exchanged in deuterated methanol. Spectra are shown in Figure S1.

β-Proteobacteria, Firmicutes, and Actinobacteria tested (see list of indicator strains in Table S1, available online). The sensitivity of *A. vinelandii* is actually not unexpected because this species should probably be reassigned to the *Pseudomonas* genus (Rediers et al., 2004; Young and Park, 2007; Özen and Ussery, 2011). For the opportunistic pathogen *Pseudomonas aeruginosa*, a larger number of environmental and clinical isolates were tested, and all 83 were found to be sensitive (Table S1). This test panel included a river isolate (Pirnay et al., 2005) and 21 representative clinical isolates (Pirnay et al., 2003, 2009) exhibiting multidrug resistances for up to 5 different antibiotic classes.

On solid medium, large inhibition halos were generated by growing or chloroform-killed RW10S1 cells, indicating secretion of a diffusible compound(s). However, only low activity was detected in culture supernatant. Therefore, the active substance was extracted from solid medium with confluent growth. The crude ethanol extract was concentrated and purified by silica gel column chromatography (preparative scale) or HPLC (analytical scale). A plate bioassay with *Pseudomonas stutzeri* as indicator was used to monitor activity. The antibacterial activity of the purified compound matched the target pattern observed for strain RW10S1, indicating that a single type of compound confers the anti-*Pseudomonas* activity. The IC_{50} values were determined for *P. aeruginosa* PA14 (0.83 ± 0.16 μg/ml; 1.75 μM), *P. syringae* pv. *glycinea* LMG 5066 (0.50 ± 0.03 μg/ml; 1.05 μM), and *P. stutzeri* LMG 2333 (0.34 ± 0.02 μg/ml; 0.71 μM). The minimal bactericidal concentrations (MBCs) were in the range of 50–150 μg/ml: *Pseudomonas savastanoi* LMG 2209 (50 μg/ml; 0.105 mM); *P. aeruginosa* PA14, *P. stutzeri* LMG 2333, *P. savastanoi* LMG 5484, and *P. syringae* pv. *glycinea* LMG 5066 (100 μg/ ml; 0.211 mM); and *P. aeruginosa* PAO1 (150 μg/ml; 0.317 mM).

Structure Elucidation

Structure elucidation was performed using a combined mass spectrometry (MS)/NMR approach. Starting with MS, the molecular composition was obtained from the accurate masses, and the general connectivity of the major parts was determined from the fragment ion spectra obtained after collision-induced dissociation. Subsequently, NMR experiments allowed for the full structural assignment of the molecule's constitution.

The peak of the protonated molecule in the full mass spectrum at *m/z* 475 indicated a mass of 474. Accurate mass determination revealed an *m/z* of 475.2766 corresponding with a composition of $C_{26}H_{39}N_2O_6$ for the protonated molecule. The fragment ion spectrum of *m/z* 475 yielded major fragments at *m/z* 114, 121, 234, 242, and 355 (Figure S1A). From this pattern it was clear that the molecule consisted of three major moieties that generated the ions at *m/z* 121, 114, and 242 and that the moiety of *m/z* 114 was located between the two other parts. A deuterium exchange experiment revealed one, two, two, and three exchangeable hydrogen atoms for the ions with *m/z* 121, 114, 234, and 242, respectively (Figure 1; Figure S1B). For the fragment ion at *m/z* 234, a third hydrogen atom was partially (33%) exchanged. Based on the accurate masses and on the results of the deuterium exchange experiments, the proposed structure can be fully supported, except for the position of the Δ^4-prolyloxy group on the 2-hydroxymyristamide moiety. This was investigated by NMR analysis and chemical transformation as described hereafter.

From the NMR spectra ($CDCl_3$ as solvent), we could immediately deduce a preliminary molecular formula of $C_{26}H_{34}NO_6$, which is in accordance with the data of the mass spectrum ($[M+H]^+$ at 475; calculated bruto formula of $C_{26}H_{39}N_2O_6$). In addition, from a ^{1}H-NMR exchange experiment with D_2O, three exchangeable protons were also detected at 9.57 ppm (typical for phenolic OH), and at 6.67 and 5.56 ppm (typical for the two hydrogens of an NH_2 amide group). Thus, the NMR data nicely underlined the MS results. Only the probably very broad signal of the secondary alcohol was not observed (see ^{1}H- and ^{13}C-NMR spectra in Figure S2).

In order to assign all the signals in the spectra (Table 1) and to deduce the sound structure for the compound, 2D-NMR experiments (COSY, GHSQC, GHMBC) were carried out, and relevant spectra are shown in Figure S2.

Combining the observed correlations with the measured 1D H,H-coupling constants and especially with the information obtained from a GHMBC or multiple-bond C,H-correlation experiment (showing long-range carbon-proton correlations over two or three bonds), we finally could propose the following structure for the new compound: a salicylic acid moiety connected via a tertiary amide bond to a Δ^4-proline whose carboxyl itself is esterified with 2,8-dihydroxymyristamide via the alcohol at position 8 (Figure 2). One of the hydroxyls of this dihydroxymyristamide is located on the α carbon (C-2), and the second oxy substituent is tentatively situated at the 8-position (C-8), mainly on the basis of the observed pattern for the ^{13}C-shifts of the remaining methylenes. However, unfortunately, the proposed position of the latter oxy substituent cannot be definitely proven due to extensive overlap of the proton signals at about 1.27 and 1.43 ppm, which precludes the use of individual and consecutive correlations.

Table 1. NMR Data ($CDCl_3$) for the RW10S1 Metabolite

Number of C	^{13}C δ (ppm)	Group[a]	^{1}H δ (ppm)	Couplings[b] (multiplets, J in Hz)
C-1	177.1	-C-	–	(amide CO)
C-2	71.1	-CH-	4.10	dd, J = 3.9 and 7.9 Hz
C-3	34.0	$-CH_2-$	1.80/1.65	m, ovl
C-4	24.4	$-CH_2-$	1.43	m, ovl
C-5	28.1	$-CH_2-$	1.27	m, ovl
C-6	24.7	$-CH_2-$	1.43/1.27	m, ovl
C-7	34.1	$-CH_2-$	1.60	m, ovl
C-8	75.8	-CH-	5.00	br, ovl
C-9	34.4	$-CH_2-$	1.60	m, ovl
C-10	25.4	$-CH_2-$	1.43/1.27	m, ovl
C-11	29.1	$-CH_2-$	1.27	m, ovl
C-12	31.7	$-CH_2-$	1.27	m, ovl
C-13	22.5	$-CH_2-$	1.27	m, ovl
C-14	14.1	$-CH_3-$	0.87	t, J = 7.0 Hz
C-15	171.2	-C-	–	(ester CO)
C-16	59.1	-CH-	5.01	dd, J = 4.6 and 11.3 Hz
C-17	33.5	$-CH_2-$	3.14 and 2.70	br dd, J = 11.3 and 17.0 Hz; br d, J = 17.0 Hz
C-18	111.0	-CH-	5.29	m
C-19	130.7	-CH-	6.71	br
C-20	167.2	-C-	–	(amide CO conjugated)
C-21	117.6	-C-	–	
C-22	157.7	-C-	–	
C-23	117.8	-CH-	6.99	dd, J = 0.9 and 8.3 Hz
C-24	133.3	-CH-	7.38	ddd, J = 1.5, 7.5, and 8.3 Hz
C-25	119.3	-CH-	6.91	dt, J = 0.9 and 7.6 Hz
C-26	128.2	-CH-	7.40	dd, J = 1.5 and 7.7 Hz
OH[c]	–	–	9.57	br, fenolic OH
NH_2[c]	–	–	6.67, 5.56	2 × br s, two amide protons
Data for 2,8-Diketomyristamide Derivative[d]				
C-1	161.8	-C-	–	(amide CO)
C-2	198.4	-C-	–	α-CO
C-3	36.3	$-CH_2-$	2.91	t, J = 7.4 Hz
C-4	22.9	$-CH_2-$	1.63	p, J = 7.5 Hz
C-5	28.6	$-CH_2-$	1.29	m, ovl
C-6	23.4	$-CH_2-$	1.54–1.61	m, ovl
C-7	42.4	$-CH_2-$	2.40	t, J = 7.4 Hz
C-8	211.3	-C-	–	CO
C-9	42.9	$-CH_2-$	2.38	t, J = 7.4 Hz
C-10	23.8	$-CH_2-$	1.54–1.61	m, ovl
C-11	28.9	$-CH_2-$	1.29	m, ovl
C-12	31.6	$-CH_2-$	1.29	m, ovl
C-13	22.5	$-CH_2-$	1.29	m, ovl
C-14	14.0	$-CH_3-$	0.88	t, J = 7.0 Hz
NH_2	–	–	5.39, 6.81	2 × br s, two amide protons

^{13}C-NMR data (chemical shift [δ]) and ^{1}H-NMR data (chemical shifts [δ] and coupling constants J [Hz]) for compound of Figure 2. Spectra are shown in Figure S2.

[a] Determined by a DEPT experiment.

[b] Coupling patterns and constants were determined from a spectrum taken at 55°C.

[c] These signals disappear from the spectrum upon addition of D_2O, and their integral value may deviate from the normal value.

[d] Assignments based on chemical shift rules and also from a GHMBC-experiment (f.i. correlation between 2.91 [H-3] with 22.9 [C4], 28.6 [C5], and 198.4 [C2]).

Therefore, final confirmation of the structure was obtained from NMR analysis of the diketomyristamide residue obtained by ester hydrolysis of promysalin and oxidation of the resulting dihydroxy derivative. The purified myristamide derivative was proven by NMR to have the proposed 2,8-diketo structure (Table 1). With respect to NMR analysis, the presence of two keto groups (at C-2 and C-x) in the myristic acid derivative divides the aliphatic chain into two isolated H,H-coupling chains, i.e., from C-3 to C-x-1, and from C-x+1 to C-14. From a HSQC-TOCSY experiment it was clearly observed that in the chain fragment correlated to H-3 (or to H-x-1), five carbons were present, and in the chain fragment correlated with H-x+1 (or with H-14), six carbons were present. This unambiguously fixes the two carbonyls in this myristamide derivative at C-2 and C-8, and definitely points to the previously proposed 2,8-dihydroxymyristic acid moiety in the promysalin. In this study no attempt was made to define the absolute configuration of the three asymmetric centers in the molecule, one in the proline part (C-16), and two in the myristamide moiety (C-2, C-8).

Being formally composed of three metabolites—a modified *pro*line residue, a *myr*istic acid derivative, and *sal*icylic acid—the trivial name promysalin is proposed for this novel, *Pseudomonas*-specific antibiotic. LC-MS analyses of cell extracts also revealed a minor amount (~1%) of a promysalin variant containing proline instead of Δ^4-proline (**1**, Figure S3). In addition the corresponding presumptive precursor molecules lacking the 2-hydroxylation of the myristic acid derivative were identified (each ~15%) (**2** and **3**, Figure S3).

Genetic Analysis of Promysalin Production

A transposon mutant library of strain RW10S1 was screened for mutants affected in promysalin production using *P. stutzeri* as indicator. In addition to 2 mutants with a reduced halo formation, 15 mutants that lacked the antibacterial activity were identified (Figure 3A; Table S2). The phenotype of the respective mutants

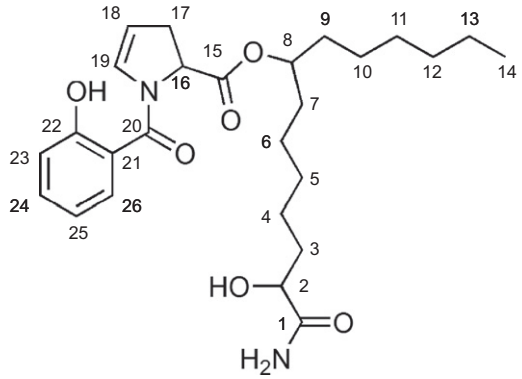

Figure 2. Structure of Promysalin

Numbering of carbon atoms for NMR assignments is indicated. In addition to promysalin, three related minor metabolites (dihydropromysalin, deoxypromysalin, dihydrodeoxypromysalin) were identified in cell extracts (see Figure S3).

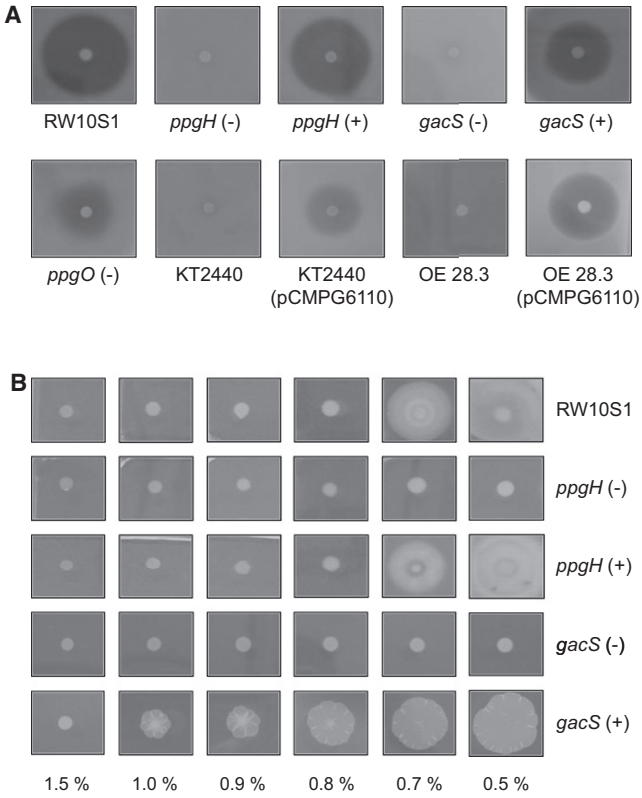

Figure 3. Phenotypes of *P. putida* RW10S1 and Representative Derived Strains

Antagonistic activity with *P. stutzeri* as overlay indicator (A) and swarming ability on media with different agar concentrations (0.5%–1.5%) (B) of RW10S1, promysalin biosynthetic mutants M-17 (insertion in *ppgH*) and M-63 (insertion in *ppgO*), and regulatory mutant M-50 (insertion in *gacS*). Minus and plus signs refer to mutants and complemented strains, respectively, using the promysalin biosynthetic region (cosmid pCMPG6110) or the subcloned *gacS* gene (shuttle vector pCMPG6113). Antibacterial activity of *P. putida* KT2440 and *P. fluorescens* OE 28.3 carrying pCMPG6110 is also shown (A). No swarming activity was conferred upon these heterologous producers (not shown). All mutants are described in Table S2.

was confirmed using other representative indicators. Because secreted amphipathic molecules can promote bacterial translocation over solid surfaces, the swarming ability of strain RW10S1 and its promysalin mutants was investigated (Figure 3B). On low-agar concentration media (below 0.8%), the wild-type strain exhibited swarming behavior. However, all mutants devoid of inhibitory activity and both mutants with reduced halo formation lost the ability of surface spreading. Biofilm formation capacity on polystyrene pegs by the mutants was reduced by one-third compared to the wild-type strain (average for nine mutants; Table S2).

Analysis of sequences flanking the respective insertion sites indicated that the *gacS* homolog was disrupted in four independent null mutants. RW10S1 genomic cosmid clone pCMPG6111, carrying *gacS*, enabled complementation of the defective inhibitory and swarming activities. Also with a subclone carrying only *gacS* in the shuttle vector pJB3Tc20 (pCMPG6113), promysalin production was restored in the *gacS* mutants (Figure 3A; Table S2). These complemented mutants displayed solid-surface translocation, but the colonies showed a mucoid phenotype, and some swarming still occurred at a higher agar concentration (up to 1%; Figure 3B). As noted in other cases, these additional morphotypic changes may be due to unbalanced plasmid-driven expression of this global regulatory component.

Complementation analysis of the non-*gacS* mutants enabled the identification of a second cosmid clone (pCMPG6110) that reintroduced promysalin-producing capacity and swarming ability, and restored biofilm formation capacity to wild-type level (Figure 3; Table S2). In addition it conferred antibacterial activity upon *Pseudomonas fluorescens* strains OE 28.3 and SBW25, and upon *P. putida* KT2440 (Figure 3A), attributable to promysalin production by HPLC analysis (results not shown). However, no swarming ability comparable to strain RW10S1 could be detected in these heterologous hosts, most likely due to additional factors required for solid-surface translocation being absent or not expressed. These observations indicated that cosmid pCMPG6110 carries (most of) the promysalin-biosynthetic genes.

Organization of the Promysalin Biosynthetic Gene Cluster

Sequencing of the pCMPG6110 insert enabled mapping of the non-*gacS* insertional mutations to a contiguous DNA region of ~15.7 kb with 13 convergent and 2 divergent ORFs (Figure 4). No equivalent or even remotely similar cluster is known for this *ppg* (*p*romysalin *p*roduction *g*enes) region in other bacteria, whereas the flanking regions display a high level of synteny to a contiguous genomic region in several *Pseudomonas*, in particular *P. putida* strains (Figure S4). Apparently, this biosynthetic cluster has been integrated near a genomic region highly conserved among *Pseudomonas* and encoding several tricarboxylic acid cycle enzymes. The G+C content of the *ppg* region differs from the flanking sequences (57.4% compared to 59.9%). However, analysis of the bordering sequences did not reveal any features reminiscent of a mobile genetic element.

The operon-like organization of the cluster was studied by RT-PCR, using RNA extracted from cells grown on solid medium.

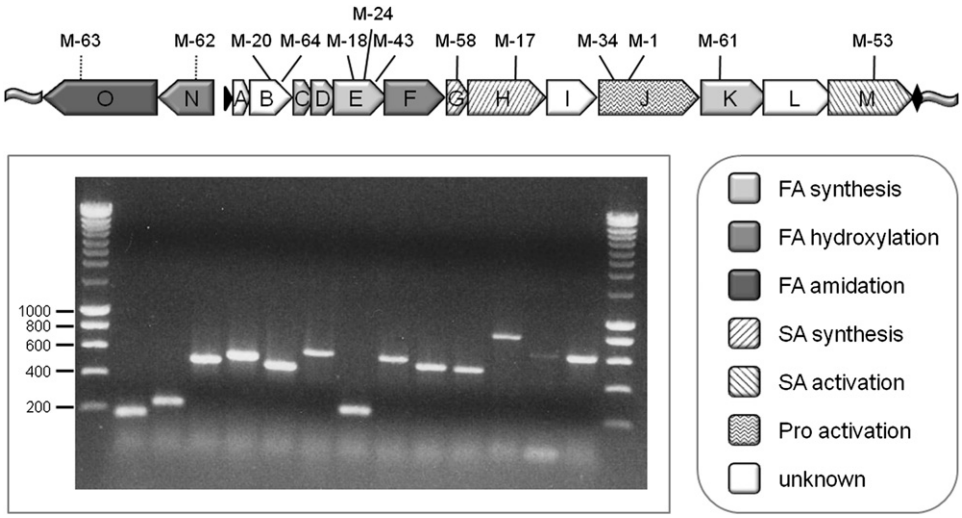

Figure 4. Organization of the Promysalin Biosynthetic Gene Cluster

Gray shading (inset) refers to predicted *ppg* gene functions (see also Table 2 and Figure 5). Plasposon insertion sites generating mutants without antagonistic activity (solid line) or mutants with reduced antagonistic activity (dashed line) are indicated. The following genes overlap: *ppgAB*, *ppgCDE*, *ppgGH*, and *ppgKLM*. A potential transcriptional ρ-independent terminator (black diamond) is indicated. Details of a putative target for translational repressor proteins of the Gac/Rsm system (black triangle) and of the syntenous regions flanking the 15.7 kb biosynthetic cluster (wavy lines) are shown in Figure S4. The agarose electrophoresis panel shows the transcript analysis by RT-PCR with primer couples for each combination of adjacent convergent gene pairs from left lane (*ppgA-ppgB*) to right lane (*ppgN-ppgO*). Size markers (bp) are indicated (see Supplemental Experimental Procedures for expected amplicon sizes). FA, fatty acid; SA, salicylic acid; Pro, proline.

All adjacent gene pairs of *ppgA* through *ppgM* as well as the *ppgN-ppgO* combination yielded amplicons of the expected size, indicating their transcriptional linkage (Figure 4). Within the *ppgA-ppgM* operon, six short overlaps of adjacent genes are present, which suggest translational coupling as well (Figure 4).

Mutant analysis indicated that promysalin is dependent on the Gac system, which typically controls expression of a subset of small RNAs that can bind to translational repressor proteins and, hence, trigger derepression of target genes (Lapouge et al., 2008). A putative target for *Pseudomonas* repressor proteins such as RsmA is present upstream of *ppgA* (Figure S4).

Deduced Functions of the Promysalin Biosynthetic Genes

The predicted amino acid sequences show only moderate-to-low similarity (<45% identity) to functionally characterized or putative gene products, mostly of diverse bacteria phylogenetically distant from the genus *Pseudomonas* (Table 2). No putative regulator or transporter genes are present. Functionally characterized homologs of PpgB and PpgI are not known, precluding assignment of a possible function. PpgB yields a poor Pfam match for the α/β-hydrolase superfamily, but secondary structure analysis predicts it with high probability to adopt a α/β-hydrolase fold. PpgI belongs to a family of as yet uncharacterized proteins exclusively encoded by proteobacterial and actinobacterial genomes (COG3687). For the other predicted gene products, a function in metabolism of the three apparent building blocks (salicylic acid, a fatty acid, proline), their assembly, and some of the tailoring activities can be proposed.

Most likely, PpgH, PpgG, and PpgM are enzymes catalyzing the conversion of chorismic acid to activated salicylic acid via isochorismic acid, mirroring the activities of equivalent enzymes in biosynthesis of the salicylic acid-containing siderophores pyochelin and pseudomonine (Gross and Loper, 2009). PpgM also shows significant similarity with actinomycete enzymes activating salicylic acid (Ishiyama et al., 2004) or methyl-substituted analogs (Van Lanen et al., 2007; Daum et al., 2009). PpgC, PpgD, PpgE, and PpgK show moderate similarity to putative type II fatty acid biosynthesis proteins from *Rhizobiales* species and other α-Proteobacteria (Table 2). However, none of the promysalin cluster genes appears to encode a homolog of β-ketoacyl-ACP reductase and enoyl-ACP reductase that catalyze the reduction steps in a complete elongation cycle (White et al., 2005). Unlike PpgK, PpgE lacks the catalytic triad of β-ketoacyl-ACP synthases (Figure S5A). This is reminiscent of the polyketide chain length factor that forms a heterodimer with the chain-elongating ketosynthase in type II polyketide synthesis (Keatinge-Clay et al., 2004). Thus, the PpgC-PpgK-PpgE triplet may be functionally equivalent to a minimal polyketide synthase complex (ACP-KSα-KSβ) (Hertweck et al., 2007).

PpgJ is composed of an adenylation (A) domain and peptidyl carrier protein (thiolation [T]) domain (with conserved serine for phosphopantetheine attachment; data not shown) but lacks the condensation (C) domain for peptide bond formation of a prototypical C-A-T extension module in nonribosomal peptide synthetase (NRPS) enzymes. The NRPSpredictor2 tool that analyzes A domain selectivity based on a 10 amino acid diagnostic motif extracted from the 34 amino acid active site signature sequence (Röttig et al., 2011) suggests that PpgJ would activate the amino acid moiety of promysalin, proline (signature: LYQAFDVSVQESFLVSAGEVNHYGPTETHVV TSY; motif: DVQFVAHVVK). The same prediction was obtained

Table 2. Characteristics of the Predicted Gene Products of the Promysalin Biosynthetic Gene Cluster

Gene	Amino Acids	Homolog, Origin (accession number)[a]	Identity/ Similarity (%)	Pfam Domain		Proposed Function
				Accession	Description	
ppgA	77	AziA5, *Streptomyces sahachiroi* (ABY83163)	40/52	PF00550	Phosphopantetheine attachment site	Carrier protein
ppgB	255	HP, *Ralstonia eutropha* (AAZ63277)	34/49	PF00561	Abhydrolase_1	?
ppgC	100	Putative ACP, *Azorhizobium caulinodans* (BAF88401.1)	32/51	PF00550	Phosphopantetheine attachment site	Acyl carrier protein
ppgD	150	Putative β-hydroxymyristoyl-ACP dehydratase, *Azorhizobium caulinodans* (BAF88402.1)	39/58	PF07977	FabA-like domain	Fatty acid synthesis
ppgE	328	Putative β-ketoacyl synthase, *Rhodopseudomonas palustris* (ABJ05965)	38/55	PF00109	β-Ketoacyl synthase, N-terminal domain	Fatty acid synthesis
ppgF	330	Putative iron-sulfur cluster-binding protein, *Thermomonospora curvata* (EEJ94718)	37/52	PF00355	Rieske [2Fe-2S] domain	Fatty acid hydroxylation
ppgG	103	Putative pyochelin biosynthetic protein, *Burkholderia cenocepacia* (CAR56091.1)	64/74	PF01817	Chorismate mutase type II	Isochorismate pyruvate lyase
ppgH	469	Putative isochorismate synthase, *Nitrococcus mobilis* (EAR23271.1)	45/60	PF00425	Chorismate-binding enzyme	Isochorismate synthase
ppgI	280	HP, marine γ-proteobacterium (EAS48157.1)	38/55	PF10118	Bacterial protein family (function unknown)	?
ppgJ	593	Putative NRPS, *Streptomyces griseus* subsp. *griseus* (BAG17413.1)	37/51	PF00501; PF00550	AMP-binding enzyme; phosphopantetheine attachment site	Proline activation
ppgK	398	Putative β-ketoacyl synthase, *Methylobacterium populi* (ACB83154.1)	39/54	PF00109; PF02801	β-Ketoacyl synthase N-terminal domain; β-ketoacyl synthase C-terminal domain	Fatty acid synthesis
ppgL	421	Hydroxycinnamoyl transferase, *Solenostemon scutellarioides* (CAK55166.1)	23/35	PF02458	Transferase family	Acyltransferase
ppgM	524	Salicylyl-AMP ligase SdgA, *Streptomyces* sp. WA46 (BAC78380.1)	43/57	PF00501	AMP-binding enzyme	Activation of salicylic acid
ppgN	332	Putative iron-sulfur cluster-binding protein, *Myxococcus xanthus* (ABF86101.1)	38/51	PF00355	Rieske [2Fe-2S] domain	Fatty acid hydroxylation[b]
ppgO	662	Putative asparagine synthase (glutamine hydrolyzing), *Pseudomonas entomophila* (CAK18134.1)	35/53	PF00310; PF00733	Glutamine amidotransferases class-II; asparagine synthase	Fatty acid amidation[b]

Multiple amino acid alignments (PpgE, PpgK, PpgL) with diagnostic motifs supporting assignments are shown in Figure S5.
[a] HP, hypothetical protein.
[b] Supported by experimental evidence.

with the PKS/NRPS analysis tool (Bachmann and Ravel, 2009). The A-T domain architecture of PpgJ indicates that it acts similarly to a NRPS loading module, selectively activating an amino acid for subsequent coupling (Bachmann and Ravel, 2009). Apparently PpgJ represents a functional equivalent of proline activation by two separate polypeptides in other systems such as the biosynthesis of prodiginines or pyoluteorin (Walsh et al., 2006; Williamson et al., 2006).

A putative T domain, distinct from the carboxy-terminal domain in PpgJ, is also present in PpgA (data not shown). No equivalent small polypeptides were detected in the databases, but significant similarity exists with peptidyl carrier domains in various NRPS enzymes. PpgA probably functions as a carrier for an (amino acid-containing) intermediate during promysalin synthesis.

The Rieske-type oxygenases PpgF and PpgN may act as monooxygenases for hydroxylation of the myristic acid part of promysalin at positions 2 and 8 (the latter being esterified in the final product). PpgO is a new member of the class II glutamine-dependent amidotransferase family (Massière and

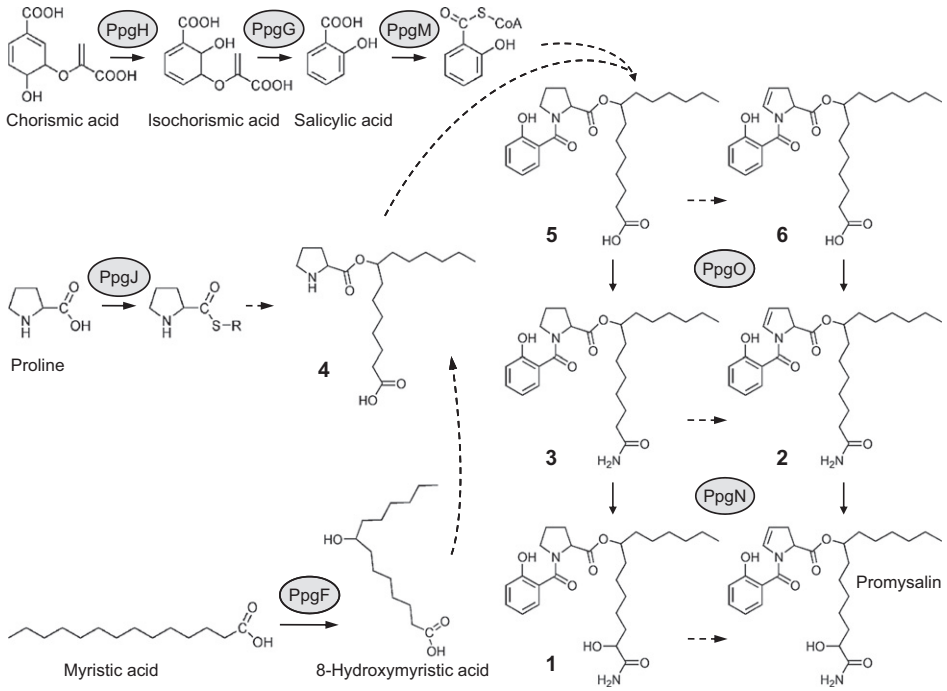

Figure 5. Proposed Pathway for Promysalin Biosynthesis

The promysalin core is assembled from proline, myristic acid, and salicylic acid. Chorismic acid serves as a salicylic acid precursor. The proposed scheme is supported by the identification of intermediates (**2–6**) arising in specific mutants (see Figure S6) and minor compounds detected in the wild-type cells (**1–3**; see Figure S3). Fatty acid biosynthesis involving PpgC, PpgD, PpgE, and PpgK is not shown. PpgA probably is a carrier for an unspecified amino acid-containing intermediate. The remaining gene products (PpgB, PpgI, PpgL) cannot be assigned to the one of the steps marked with dashed arrows.

Badet-Denisot, 1998). These enzymes transfer an amido-nitrogen from glutamine to diverse acceptors, as demonstrated for biosynthesis of fredericamycin A (FdmV) (Chen et al., 2010) or thiostrepton A (TsrT) (Kelly et al., 2009) by *Streptomyces* species. Therefore, PpgO is likely involved in amidation of the fatty acid moiety of promysalin. PpgL shows very low similarity (<25% identity) to members of the BAHD superfamily, a divergent family of plant enzymes using CoA-activated molecules to *N*- or *O*-acylate very diverse substrates (D'Auria, 2006) (Figure S5B).

Identification of Biosynthetic Intermediates

A tentative scheme for biosynthesis of promysalin based on bioinformatic analysis and identification of some intermediates in particular mutants is shown in Figure 5. In the *ppgM* transposon mutant, presumably unable to activate salicylic acid, a biosynthetic intermediate consisting of proline esterified with 8-hydroxymyristic acid (**4**) was identified (Figure S6A). This indicates that the 8-hydroxyl group is introduced before conjugation with salicylic acid. To investigate the possibility that the predicted transferase PpgL may be involved in producing compound **4** or in its subsequent coupling to salicylic acid, an unmarked nonpolar mutant lacking *ppgL* (CMPG2117) was constructed, excluding a possible polar effect on *ppgM* expression. This provided no further clue about the role of PpgL because the mutant lacked antibacterial activity, but no promysalin-related intermediate could be detected (data not shown).

The salicylyl conjugate (**5**) was identified in both *ppgN* and *ppgO* transposon mutants, in addition to the equivalent molecule with Δ^4-proline instead of proline (**6**) (Figures S6B and S6C). To elucidate the role of PpgN and PpgO in further modification of the conjugated fatty acid, an unmarked nonpolar *ppgN* mutant, retaining *ppgO*-dependent activity, was generated. In this mutant (CMPG2118), which equally displayed residual antibacterial activity, the respective amidated precursors of promysalin (**2**) and of dihydropromysalin (**3**) were detected (Figure S6D), demonstrating that amidation by PpgO precedes the final 2-hydroxylation step requiring PpgN (Figure 5). Additional intermediates detected for CMPG2118 (**5**, **6**) point to accumulation of precursors by blocking the PpgN-dependent step.

DISCUSSION

Promysalin represents a novel type of amphipathic salicylic acid-containing antibiotic with unusual intragenus specificity, synthesized from three different central metabolites through the action of a hitherto unreported combination of gene products. To our knowledge, no comparable (antimicrobial) molecules have been identified in other organisms. Some superficial similarity exists with the antifungal compound salaceyin A, a 6-alkyl-substituted salicylic acid derivative produced by the actinomycete *Streptomyces laceyi* (Park et al., 2007), and with antibacterial 6-alk(en)ylsalicylic acids (anacardic acids) isolated from some plants (Kubo et al., 2003; Choi et al., 2009). Several bacteria synthesize salicylic acid (2-hydroxybenzoic acid) for incorporation in siderophores like anachelin 1 (*Anabaena*), pyochelin (*Pseudomonas*, *Burkholderia*), vulnibactin (*Vibrio*),

yersiniabactin (*Yersinia*), or mycobactin (*Mycobacterium*), with the carboxylic group integrated in a 2-thiazoline or 2-oxazoline moiety, and anachelin H (*Anabaena*) or pseudomonine (*Pseudomonas*), with an amide-linked carboxylic group (Ferreras et al., 2005; Rastogi and Sinha, 2009; Gross and Loper, 2009). However, unlike such iron-capturing metabolites, promysalin is produced in rich, iron-sufficient medium and apparently serves other functions. The dependence on a functional *gacS* gene of promysalin production is in line with this, as discussed below.

GacS is the sensor of the GacS/GacA two-component regulatory system that modulates "social" behavior in different γ-Proteobacteria, including production of virulence factors, antimicrobial metabolites, biosurfactants, and control of (swarming) motility (Lapouge et al., 2008). In combining *Pseudomonas*-antagonizing activity with promotion of biofilm formation and surface spreading, the ecological role of this secondary metabolite may lie in facilitating colonization by its producer of structured environments equally preferred by many other pseudomonads, such as the rhizosphere, relying on a conquer-and-kill strategy. Notably, promysalin is produced by a *P. putida* strain originally isolated from rice roots (Vlassak et al., 1992). Quorum sensing mediated by *N*-acyl homoserine lactones is involved in the cell density-dependent production by rhizosphere-colonizing *Pseudomonas* of some antifungal secondary metabolites such as phenazines (Haas and Défago, 2005). The fact that no quorum-sensing mutants affected in promysalin production were identified in this study is consistent with the failure to identify *N*-acyl homoserine lactone production by wild-type strain RW10S1 (Steindler et al., 2008).

Promysalin contains two unique moieties (2-pyrroline-5-carboxylic acid and 2,8-dihydroxymyristamide) not previously described in a (secondary) metabolite. Therefore, it is not surprising that the promysalin biosynthetic gene set lacks an equivalent in other bacteria, apart from three genes for salicylic acid biosynthesis and activation. The *ppg* cluster seems to have evolved from a mosaic assembly of genes recruited from different metabolic pathways in diverse, mostly phylogenetically distant or unrelated organisms. Gene product functional predictions combined with identification of intermediates in some of the biosynthetic mutants allow us to propose a possible route for assembly of promysalin from chorismic acid (being converted to salicylic acid), an amino acid (proline), and a fatty acid (myristic acid) (Figure 5). It will be of particular interest to elucidate the activity of PpgL in this because no other bacterial BAHD-type transferase has been characterized yet. Further genetic and biochemical dissection of this novel pathway may reveal other interesting novel biocatalytic activities, such as the unusual fatty acid ω-7 hydroxylation. It appears that proline, and not its immediate anabolic precursor 1-pyrroline-5-carboxylate, is incorporated and subsequently converted to the 2-pyrroline ring present in promysalin.

Elucidation of the mode of action of promysalin may provide insight into its selective toxicity for *Pseudomonas*. This kind of intragenus antagonism is typical for bacteriocins but unusual for secondary metabolites. The possible effects of promysalin on colonized plants also deserve further attention, in view of the important role played by salicylic acid in plant defense signaling (Vlot et al., 2009) and its capacity to interfere with bacterial quorum-sensing systems (Yuan et al., 2008; Yang et al., 2009). Synthetic analogs with systematically modified building blocks will be valuable for determining structure-activity relationship in such studies.

SIGNIFICANCE

The identification of the antagonistic and surface colonization-promoting secondary metabolite promysalin discloses another physiological role for a salicylic acid derivative in bacteria. In phylogenetically unrelated species, salicylic acid is synthesized as a building block for diverse siderophores (anachelin, mycobactin, pseudomonine, pyochelin, yersiniabactin, vulnibactin), produced under iron-limiting conditions. However, production of salicylic acid-containing promysalin is not triggered by low-iron availability but is dependent on the Gac/Rsm regulatory system that controls a variety of "social" functions in γ-Proteobacteria, including motility and antagonism of microbial competitors. Being produced by a rice root-associated *Pseudomonas* strain, promysalin may contribute to aggressive colonization of structured environments such as the nutrient-enriched rhizosphere of plants, in competition with other pseudomonads. Additional physiological effects potentially exerted by promysalin that deserve further scrutiny relate to its apparent role in biofilm formation, the ability of its constituent salicylic acid to interfere with bacterial quorum sensing, and the key role of salicylic acid as a signaling molecule in induced defense of plants against invading organisms.

Promysalin displays a remarkable antagonistic spectrum, selectively targeting other pseudomonads, including multidrug-resistant clinical isolates of the major opportunistic human pathogen *P. aeruginosa*. Further study of the mode of action of this compound and structure-activity relationship for analogs may reveal a useful antibiotic target. The compound is composed of salicylic acid and a fatty acid derivative (2,8-dihydroxymyristamide) connected by a 2-pyrroline-5-carboxyl moiety. Characterization of the biosynthetic gene cluster and identification of some intermediates revealed a pathway involving several biosynthetic activities for recruiting precursors from fatty acid and proline metabolism and converting these to unusual building blocks. Notably, one of the biosynthetic genes appears to encode a prokaryotic member in the BAHD family of plant-specific acyltransferases, and may have evolved from a horizontally acquired plant gene.

EXPERIMENTAL PROCEDURES

Bacterial Strains, Plasmids, and Culture Conditions

Bacterial strains and plasmids used are described in the Supplemental Experimental Procedures. Standard methods for growth and manipulation of *E. coli* were used (Sambrook and Russell, 2001). Trypticase soy broth (TSB) medium was used for routine culturing of *Pseudomonas* at 30°C or 37°C (for *P. aeruginosa*). Antagonistic activity was detected using an agar diffusion assay (Parret et al., 2003). Conjugative transfer of shuttle plasmids and cosmids to *Pseudomonas* strains was achieved by triparental conjugation using *E. coli* HB101 bearing pRK2013 as helper strain (Ditta et al., 1980). MBC values were determined in TSB medium according to Andrews (2001). For IC_{50} determination, growth inhibition patterns of *Pseudomonas* strains in TSB with

different antibiotic concentrations (in triplicate) were monitored in a Bioscreen C growth analyzer (Oy Growth Curves Ab). The average IC_{50} was determined at time points 16, 18, and 20 hr. Swarming ability was studied by spotting 5 μl of overnight-grown cells on TSB agar (concentration range, 0.5%–1.5%) and evaluating surface spreading after incubation at 30°C for 16–24 hr. Biofilm formation was assayed at 25°C according to Janssens et al. (2008).

Purification of Antibiotic

An overnight TSB culture of strain RW10S1 (8 ml) was mixed with 2.4 liters of liquefied medium (TSB containing 1% agar) and poured into Petri dishes (~16 ml of medium/plate). After 16–24 hr incubation at 30°C, medium with confluent growth of bacteria was mixed with an equal volume of 100% ethanol for 15 min, and the extract was clarified by centrifugation (twice at 9000 × g; 25 min; 4°C). The crude extract was concentrated 5- to 10-fold by rotavap at 50°C and stored at 4°C till further use. To monitor activity during purification, the plate bioassay was used with *P. stutzeri* as indicator.

Analytical HPLC purification (Agilent 1100) was used to compare antibiotic production in different strains. Samples for HPLC (~35 ml) were prepurified using ISOLUTE SPE columns (C8-EC; Sopachem) and then purified by the Microsorb-MV C8 HPLC column (300 Å pore size, 250 × 4.6 mm; Varian) with a linear acetonitrile/water gradient. Preparative-scale purification was carried out by silica gel column chromatography with a dichloromethane/methanol mixture (95:5 v/v). Absorbance measurements were used to determine concentration of samples for subsequent analyses (λ_{max} = 280 nm, ε = 6714 l mol^{-1} cm^{-1}; purified compound dissolved in methanol). In a typical purification procedure, about 12.5 mg of purified compound was obtained from 150 plates (see Supplemental Experimental Procedures for details).

Structure Elucidation by MS and NMR

MS was performed on a quadrupole orthogonal acceleration time-of-flight mass spectrometer (Q-Tof-2; Micromass) equipped with a standard electrospray probe (Z-spray; Micromass). For the MS/MS spectra the accurate mass of the precursor ion was used as lock mass. Deuterium exchange spectra were obtained by evaporating and redissolving the samples twice in methanol-d (Janssen Chimica). ^{1}H- and ^{13}C-NMR spectra were recorded on a Bruker Avance II 600 spectrometer operating at 600.130 MHz for ^{1}H and at 150.903 MHz for ^{13}C, and using a gradient-equipped inverse 5 mm triple probe with $\pi/2$ pulses of 10.5 and 11.5 μs, respectively. The standard Bruker Topspin 2.1 software under Windows XP was used throughout. For confirming the position of the second oxy substituent, dihydroxymyristamide was released by ester hydrolysis of promysalin with 1 M NaOH and oxidized to diketomyristamide by a Jones oxidation with chromic acid, then applied to NMR analysis (see Supplemental Experimental Procedures for more details).

Mutant Library Construction and Screening

A RW10S1 mutant library was constructed using transposon pTn*Mod*-OKm' introduced by electroporation (Dennis and Zylstra, 1998). Efficient transformation required the use of nonmethylated plasmid DNA, obtained by propagation of pTn*Mod*-OKm' in the methylation-deficient *E. coli* strain GM2163 (Parret et al., 2003). The library was screened for mutants with abolished or reduced activity against *P. stutzeri* by the agar diffusion method, using a 6 column × 8 row array of clones in square Petri dishes (12 × 12 cm). Confirmed activity mutants were subjected to plasposon rescue (Dennis and Zylstra, 1998). Transposon-flanking DNA sequences in the respective rescued plasmids were determined using two outward-reading pTn*Mod*-OKm'-specific primers.

Construction of Unmarked Deletion Mutants

Mutants lacking the entire coding region of *ppgL* (CMPG2117) or *ppgN* (CMPG2118) were constructed by double homologous recombination using suicide vector pAKE604, carrying a DNA fragment assembled from PCR-amplified regions upstream and downstream of the target gene (Mattheus et al., 2010). Primer sequences are listed in the Supplemental Experimental Procedures. Nonpolarity of the mutations was confirmed by detection of expression of the respective downstream genes using RT-PCR.

Genomic Cosmid Library Construction and Screening

Total DNA of strain RW10S1 was partially restricted with *Sau*3AI and cloned in *Bam*HI-cut pRG930-Cm^{R}. The ligated DNA was packaged using the Gigapack III Gold-4 kit (Stratagene) and transformed in *E. coli* VCS257. PCR screening with primer combinations designed from Tn*Mod*-flanking sequences in mutants was used to identify a template clone (pCMPG6110) that enabled amplification of most target genes. The insert sequence was determined by a combination of subcloning and primer walking. The same strategy was used to identify a cosmid clone (pCMPG6111) carrying *gacS*. The *gacS* and flanking sequences were determined by primer walking. The 3655-bp *gacS*-containing fragment obtained from *Hin*dIII-digested pCMPG6111 was cloned into shuttle vector pJB3Tc20 generating pCMPG6113.

RNA Extraction and RT-PCR

Total RNA was isolated from RW10S1 cells after 20 hr of growth on TSB agar plate, using the TRIzol Plus RNA Purification System protocol (Invitrogen). RNA samples were treated with TURBO DNA-*free* Kit (Ambion) to remove contaminating genomic DNA. RNA was quantified using the NanoDrop ND-1000 system (Thermo Scientific). First-strand cDNA was synthesized using Random Decamers (50 μM; Ambion), M-MuLV Reverse Transcriptase (Westburg), and dNTP set (Westburg), and subsequently used as a template for RT-PCR with specific primers using Taq polymerase (Biolabs). Primer sequences are listed in the Supplemental Experimental Procedures.

ACCESSION NUMBERS

The nucleotide sequences reported in this paper are available in GenBank under accession numbers GU211009 (*gacS*) and GU211010 (*ppg* cluster).

SUPPLEMENTAL INFORMATION

Supplemental Information includes six figures, two tables, and Supplemental Experimental Procedures and can be found with this article online at doi:10.1016/j.chembiol.2011.08.006.

ACKNOWLEDGMENTS

This work was supported by Grant G.0303.04N from FWO-Vlaanderen (to P.C. and R.DM.), by a K.U.Leuven-Zhejiang University interuniversity SBA fellowship to W.L. (K.U.Leuven Research Council Fund), and by a junior postdoctoral fellowship F/04/026-F/05/32 to P.E-dlS. (K.U.Leuven Research Council Fund). The authors thank Sarah Denayer and Hassan Rokni-Zadeh for antagonism assays with *P. aeruginosa* and *P. savastanoi*, respectively, and Wesley Mattheus for advice on construction of unmarked deletion mutants. The assistance of Luc Baudemprez for recording NMR spectra and Xiaoping Song with chemical analyses is much appreciated. Guido Bloemberg kindly provided plasmid pMP6562.

Received: November 19, 2009
Revised: June 15, 2011
Accepted: August 2, 2011
Published: October 27, 2011

REFERENCES

Andrews, J.M. (2001). Determination of minimum inhibitory concentrations. J. Antimicrob. Chemother. *48* (*Suppl 1*), 5–16.

Bachmann, B.O., and Ravel, J. (2009). Chapter 8. Methods for in silico prediction of microbial polyketide and nonribosomal peptide biosynthetic pathways from DNA sequence data. Methods Enzymol. *458*, 181–217.

Barreteau, H., Bouhss, A., Fourgeaud, M., Mainardi, J.L., Touzé, T., Gérard, F., Blanot, D., Arthur, M., and Mengin-Lecreulx, D. (2009). Human- and plant-pathogenic *Pseudomonas* species produce bacteriocins exhibiting colicin M-like hydrolase activity towards peptidoglycan precursors. J. Bacteriol. *191*, 3657–3664.

Braun, S.D., Hofmann, J., Wensing, A., Ullrich, M.S., Weingart, H., Völksch, B., and Spiteller, D. (2010). Identification of the biosynthetic gene cluster for 3-methylarginine, a toxin produced by *Pseudomonas syringae* pv. syringae 22d/93. Appl. Environ. Microbiol. *76*, 2500–2508.

Chen, Y., Wendt-Pienkowski, E., Ju, J., Lin, S., Rajski, S.R., and Shen, B. (2010). Characterization of FdmV as an amide synthetase for fredericamycin A biosynthesis in *Streptomyces griseus* ATCC 43944. J. Biol. Chem. *285*, 38853–38860.

Choi, J.G., Jeong, S.I., Ku, C.S., Sathishkumar, M., Lee, J.J., Mun, S.P., and Kim, S.M. (2009). Antibacterial activity of hydroxyalkenyl salicylic acids from sarcotesta of *Ginkgo biloba* against vancomycin-resistant *Enterococcus*. Fitoterapia *80*, 18–20.

Daum, M., Peintner, I., Linnenbrink, A., Frerich, A., Weber, M., Paululat, T., and Bechthold, A. (2009). Organisation of the biosynthetic gene cluster and tailoring enzymes in the biosynthesis of the tetracyclic quinone glycoside antibiotic polyketomycin. ChemBioChem *10*, 1073–1083.

D'Auria, J.C. (2006). Acyltransferases in plants: a good time to be BAHD. Curr. Opin. Plant Biol. *9*, 331–340.

Dennis, J.J., and Zylstra, G.J. (1998). Plasposons: modular self-cloning minitransposon derivatives for rapid genetic analysis of gram-negative bacterial genomes. Appl. Environ. Microbiol. *64*, 2710–2715.

Ditta, G., Stanfield, S., Corbin, D., and Helinski, D.R. (1980). Broad host range DNA cloning system for gram-negative bacteria: construction of a gene bank of *Rhizobium meliloti*. Proc. Natl. Acad. Sci. USA *77*, 7347–7351.

Ferreras, J.A., Ryu, J.-S., Di Lello, F., Tan, D.S., and Quadri, L.E.N. (2005). Small-molecule inhibition of siderophore biosynthesis in *Mycobacterium tuberculosis* and *Yersinia pestis*. Nat. Chem. Biol. *1*, 29–32.

Gross, H., and Loper, J.E. (2009). Genomics of secondary metabolite production by *Pseudomonas* spp. Nat. Prod. Rep. *26*, 1408–1446.

Haas, D., and Défago, G. (2005). Biological control of soil-borne pathogens by fluorescent pseudomonads. Nat. Rev. Microbiol. *3*, 307–319.

Hertweck, C., Luzhetskyy, A., Rebets, Y., and Bechthold, A. (2007). Type II polyketide synthases: gaining a deeper insight into enzymatic teamwork. Nat. Prod. Rep. *24*, 162–190.

Inglis, R.F., Gardner, A., Cornelis, P., and Buckling, A. (2009). Spite and virulence in the bacterium *Pseudomonas aeruginosa*. Proc. Natl. Acad. Sci. USA *106*, 5703–5707.

Ishiyama, D., Vujaklija, D., and Davies, J. (2004). Novel pathway of salicylate degradation by *Streptomyces* sp. strain WA46. Appl. Environ. Microbiol. *70*, 1297–1306.

Janssens, J.C., Steenackers, H., Robijns, S., Gellens, E., Levin, J., Zhao, H., Hermans, K., De Coster, D., Verhoeven, T.L., Marchal, K., et al. (2008). Brominated furanones inhibit biofilm formation by *Salmonella enterica* serovar Typhimurium. Appl. Environ. Microbiol. *74*, 6639–6648.

Keatinge-Clay, A.T., Maltby, D.A., Medzihradszky, K.F., Khosla, C., and Stroud, R.M. (2004). An antibiotic factory caught in action. Nat. Struct. Mol. Biol. *11*, 888–893.

Kelly, W.L., Pan, L., and Li, C. (2009). Thiostrepton biosynthesis: prototype for a new family of bacteriocins. J. Am. Chem. Soc. *131*, 4327–4334.

Kubo, I., Nihei, K., and Tsujimoto, K. (2003). Antibacterial action of anacardic acids against methicillin resistant *Staphylococcus aureus* (MRSA). J. Agric. Food Chem. *51*, 7624–7628.

Lapouge, K., Schubert, M., Allain, F.H., and Haas, D. (2008). Gac/Rsm signal transduction pathway of γ-proteobacteria: from RNA recognition to regulation of social behaviour. Mol. Microbiol. *67*, 241–253.

Ligon, J.M., Hill, D.S., Hammer, P.E., Torkewitz, N.R., Hofmann, D., Kempf, H.-J., and van Pée, K.-H. (2000). Natural products with antifungal activity from *Pseudomonas* biocontrol bacteria. Pest Manag. Sci. *56*, 688–695.

Massière, F., and Badet-Denisot, M.A. (1998). The mechanism of glutamine-dependent amidotransferases. Cell. Mol. Life Sci. *54*, 205–222.

Mattheus, W., Gao, L.-J., Herdewijn, P., Landuyt, B., Verhaegen, J., Masschelein, J., Volckaert, G., and Lavigne, R. (2010). Isolation and purification of a new kalimantacin/batumin-related polyketide antibiotic and elucidation of its biosynthesis gene cluster. Chem. Biol. *17*, 149–159.

Michel-Briand, Y., and Baysse, C. (2002). The pyocins of *Pseudomonas aeruginosa*. Biochimie *84*, 499–510.

Özen, A.I., and Ussery, D.W. (2011). Defining the *Pseudomonas* genus: where do we draw the line with *Azotobacter*? Microb. Ecol., in press. Published online August 3, 2011. 10.1007/s00248-011-9914-8.

Park, C.N., Lee, D., Kim, W., Hong, Y., Ahn, J.S., and Kim, B.S. (2007). Antifungal activity of salaceyin A against *Colletotrichum orbiculare* and *Phytophthora capsici*. J. Basic Microbiol. *47*, 332–339.

Parret, A.H.A., Temmerman, K., and De Mot, R. (2005). Novel lectin-like bacteriocins of biocontrol strain *Pseudomonas fluorescens* Pf-5. Appl. Environ. Microbiol. *71*, 5197–5207.

Parret, A.H.A., Schoofs, G., Proost, P., and De Mot, R. (2003). Plant lectin-like bacteriocin from a rhizosphere-colonizing *Pseudomonas* isolate. J. Bacteriol. *185*, 897–908.

Pirnay, J.P., De Vos, D., Cochez, C., Bilocq, F., Pirson, J., Struelens, M., Duinslaeger, L., Cornelis, P., Zizi, M., and Vanderkelen, A. (2003). Molecular epidemiology of *Pseudomonas aeruginosa* colonization in a burn unit: persistence of a multidrug-resistant clone and a silver sulfadiazine-resistant clone. J. Clin. Microbiol. *41*, 1192–1202.

Pirnay, J.P., Matthijs, S., Colak, H., Chablain, P., Bilocq, F., Van Eldere, J., De Vos, D., Zizi, M., Triest, L., and Cornelis, P. (2005). Global *Pseudomonas aeruginosa* biodiversity as reflected in a Belgian river. Environ. Microbiol. *7*, 969–980.

Pirnay, J.P., Bilocq, F., Pot, B., Cornelis, P., Zizi, M., Van Eldere, J., Deschaght, P., Vaneechoutte, M., Jennes, S., Pitt, T., and De Vos, D. (2009). *Pseudomonas aeruginosa* population structure revisited. PLoS One *4*, e7740.

Raaijmakers, J.M., De Bruijn, I., Nybroe, O., and Ongena, M. (2010). Natural functions of lipopeptides from *Bacillus* and *Pseudomonas*: more than surfactants and antibiotics. FEMS Microbiol. Rev. *34*, 1037–1062.

Rastogi, R.P., and Sinha, R.P. (2009). Biotechnological and industrial significance of cyanobacterial secondary metabolites. Biotechnol. Adv. *27*, 521–539.

Rediers, H., Vanderleyden, J., and De Mot, R. (2004). *Azotobacter vinelandii*: a *Pseudomonas* in disguise? Microbiology *150*, 1117–1119.

Röttig, M., Medema, M.H., Blin, K., Weber, T., Rausch, C., and Kohlbacher, O. (2011). NRPSpredictor2—a web server for predicting NRPS adenylation domain specificity. Nucleic Acids Res. *39*, W362–W367.

Sambrook, J., and Russell, D.W. (2001). Molecular Cloning: A Laboratory Manual, Third Edition (Cold Spring Harbor, NY: Cold Spring Harbor Laboratory).

Srinivas, N., Jetter, P., Ueberbacher, B.J., Werneburg, M., Zerbe, K., Steinmann, J., Van der Meijden, B., Bernardini, F., Lederer, A., Dias, R.L., et al. (2010). Peptidomimetic antibiotics target outer-membrane biogenesis in *Pseudomonas aeruginosa*. Science *327*, 1010–1013.

Steindler, L., Bertani, I., De Sordi, L., Bigirimana, J., and Venturi, V. (2008). The presence, type and role of *N*-acyl homoserine lactone quorum sensing in fluorescent *Pseudomonas* originally isolated from rice rhizospheres are unpredictable. FEMS Microbiol. Lett. *288*, 102–111.

Thomas, C.M., Hothersall, J., Willis, C.L., and Simpson, T.J. (2010). Resistance to and synthesis of the antibiotic mupirocin. Nat. Rev. Microbiol. *8*, 281–289.

Van Lanen, S.G., Oh, T.-J., Liu, W., Wendt-Pienkowski, E., and Shen, B. (2007). Characterization of the maduropeptin biosynthetic gene cluster from *Actinomadura madurae* ATCC 39144 supporting a unifying paradigm for enediyne biosynthesis. J. Am. Chem. Soc. *129*, 13082–13094.

Vlassak, K., Holm, L., Duchateau, L., Vanderleyden, J., and De Mot, R. (1992). Isolation and characterization of fluorescent *Pseudomonas* associated with the roots of rice and banana grown in Sri Lanka. Plant Soil *145*, 51–63.

Vlot, A.C., Dempsey, D.A., and Klessig, D.F. (2009). Salicylic acid, a multifaceted hormone to combat disease. Annu. Rev. Phytopathol. *47*, 177–206.

Waite, R.D., and Curtis, M.A. (2009). *Pseudomonas aeruginosa* PAO1 pyocin production affects population dynamics within mixed-culture biofilms. J. Bacteriol. *191*, 1349–1354.

Walsh, C.T., Garneau-Tsodikova, S., and Howard-Jones, A.R. (2006). Biological formation of pyrroles: nature's logic and enzymatic machinery. Nat. Prod. Rep. *23*, 517–531.

White, S.W., Zheng, J., Zhang, Y.M., and Rock, C.O. (2005). The structural biology of type II fatty acid biosynthesis. Annu. Rev. Biochem. *74*, 791–831.

Williamson, N.R., Fineran, P.C., Leeper, F.J., and Salmond, G.P.C. (2006). The biosynthesis and regulation of bacterial prodiginines. Nat. Rev. Microbiol. *4*, 887–899.

Yang, L., Rybtke, M.T., Jakobsen, T.H., Hentzer, M., Bjarnsholt, T., Givskov, M., and Tolker-Nielsen, T. (2009). Computer-aided identification of recognized drugs as *Pseudomonas aeruginosa* quorum-sensing inhibitors. Antimicrob. Agents Chemother. *53*, 2432–2443.

Young, J.M., and Park, D.C. (2007). Probable synonymy of the nitrogen-fixing genus *Azotobacter* and the genus *Pseudomonas*. Int. J. Syst. Evol. Microbiol. *57*, 2894–2901.

Yuan, Z.C., Haudecoeur, E., Faure, D., Kerr, K.F., and Nester, E.W. (2008). Comparative transcriptome analysis of *Agrobacterium tumefaciens* in response to plant signal salicylic acid, indole-3-acetic acid and gamma-amino butyric acid reveals signalling cross-talk and *Agrobacterium*—plant co-evolution. Cell. Microbiol. *10*, 2339–2354.

